# Numerical Study of Regional Climate

Wen-Yih Sun, Jiun-Dar Chern, and Michael Bosilovich

Department of Earth and Atmospheric Sciences
Purdue University
West Lafayette, IN 47907-1397

## Abstract

*During the summer of 1988, severe drought caused extensive loss of crops in the midwestern United States. A high resolution physically comprehensive atmospheric numerical model (Purdue Mesoscale Model, PMM) is integrated for the thirty days of June 1988. The preliminary results show the PMM can reproduce the observed weather pattern of June 1988 very well. It is also proved that this model can be an important tool to study the regional climate change and water cycle in a time scale of month over a large continent.*

## 1. Introduction

The drought of 1988 over the Midwest and Gulf States of the USA (Fig. 1) had caused severe damage in agriculture, transportation and other resources. Although many scientists have worked on this problem, the cause of the drought is still unclear. The existing operational numerical weather prediction models failed to predict the 1988 drought or the 1993 flood in Mississippi Valley, which also caused casualty of life and the tremendous lost in agriculture and property.

Since flood or drought can threaten most place around the world, an accurate long-range weather forecasting will be crucial in order to reduce the lost of life and properties due to the extreme weather phenomena. Here, we apply the Purdue Mesoscale Model (PMM) to simulate the evolution of the weather during June of 1988. The thirty days simulations show that with an appropriate initial and lateral boundary conditions, the PMM is capable of reproducing the observed weather pattern reasonably well. Furthermore, the PMM can produce a complete data set in both space and time to study the detailed evolution of the weather as well as the hydrological cycle. We can also test different forcing (or parameter) in a numerical model in order to evaluate the importance of that particular forcing (or parameter). Hence, the PMM can become an important tool to study the changes of regional climate.

## 2. Purdue Mesoscale Model

### 2.A Basic Equations and Physics

The model is based on the hydrostatic approximation in a terrain-following sigma-p ($\sigma$) coordinate. Here, $\sigma$ is defined as

$$\sigma = (p-p_t)/(p_s-p_t) = (p-p_t)/p_*$$

where, p, $p_s$ and $p_t$ are the pressure, the surface pressure, and the pressure at the top of the model, respectively. There are ten prognostic equations in the model for ten primary variables:

$\theta_e$ (the equivalent potential temperature),

$q_w$ (the total water content $q_w$ ; $q_w = q_v$ (water vapor mixing ratio) + $q_l$( cloud water mixing ratio) ),

u and v (the horizontal components of wind),

$p_*$ ( = $p_s$ - $p_t$ ),

TKE (turbulent kinetic energy),

$T_{sfc}$ (surface soil temperature),

$w_{sfc}$ (surface soil moisture).

$T_2$ (temperature inside the soil), and

$w_2$ (water content inside the soil).

The general form of those nonlinear partial differential equations can be expressed as:

$$\frac{\partial \varphi}{\partial t} = -u\frac{\partial \varphi}{\partial x} - v\frac{\partial \varphi}{\partial x} - \dot{\sigma}\frac{\partial \varphi}{\partial \sigma} - souce(\varphi) + diff(\varphi) \qquad (1)$$

where u=dx/dt, v=dy/dt, and $\dot{\sigma}$=d$\sigma$/dt are velocity along the x, y and $\sigma$ coordinate, respectively; source($\varphi$) is the source or sink of $\varphi$; diff($\varphi$) is the diffusion. It is noted that there is no advection terms for equations of $T_{sfc}$, $w_{sfc}$, $T_2$, and $w_2$. The equation of conservation of mass is given by

$$\frac{\partial p_*}{\partial t} = -\int_0^1 \nabla_\sigma \cdot (p_* v)\, d\sigma \qquad (2)$$

In addition to the prognostic equations, there are several diagnostic equations in the model to compute some diagnostic variables, for example, the velocity $\dot{\sigma}$ along the $\sigma$-coordinate, pressure, temperature, water vapor, and eddy-diffusion coefficients. The details of those equations can be found in [1], [2], and [3]. The physics of atmosphere have been parameterized in the model, these includes:

(a) the surface budget equations for heat and moisture with or without vegetation [4] ;

(b) similarity equations at the constant flux layer [5] ;

(c) the turbulence parameterizations and eddy fluxes in the planetary boundary layer ([6] and [7]) ;

(d) the short-and long-wave radiations for both inside and outside the cloud ([8] and [9]) ;

(e) the phase change of water substance and diabatic heating [10] ;

(f) cumulus parameterization ([11] and 12) ;

(h) the observed sea surface temperature is used over the ocean.

## 2.B Numerical Method and Experimental Designs

A time-splitting scheme is used in the integration of the governing equation. It allows the application of different numerical methods and time intervals to different terms or groups of terms in the governing equations ([13] and [10]). A small time interval with a forward-backward scheme ([14] and [15]) is applied to the terms involving inertia-gravity waves. This scheme not only allows twice the time interval used in the leapfrog scheme, but also avoids the $2\Delta t$ waves that usually exist in a central-difference scheme in time. Another time interval, $\Delta t_b$, limited by the horizontal advection, is applied to the horizontal advection, the diffusion terms and surface budget equations. The radiation is calculated every 30

minutes. We also use a local reference to calculate the pressure gradient terms, as suggested by [16] in order to avoid the huge errors over the mountain areas. The advection scheme developed by [17] is applied in this model.

The Arakawa C staggered grid is chosen in this model. The domain has 25 vertical layers from the surface up to 100 mb. A stretched grid is used in the vertical direction in order to have better resolution in the lower atmosphere. In this study, the interior area of the horizontal domain is about 6000 x 4500 $km^2$, consisting of 100 x 75 grid points with horizontal grid interval of $\Delta x = \Delta y = 60$ km, which is surrounded by a buffer zone with a much larger space interval ($\geq 6\Delta x$) to reduce the reflection and uncertainty around the lateral boundary. Newtonian damping is applied to the top five layers in order to avoid reflection of the waves from the top. A weak horizontal smoothing is also applied in the prognostic equations to avoid nonlinear instability. The details of the numerical method can be found in [1], [2] and [3].

This model has been applied to simulate the cold air outbreak and cellular convection over the Kuroshio Current ([10] and [18]), lee -vortexes and mesolow in Taiwan ([1], [19] and [20]); the low-level jet (LLJ) and moisture convergence for Taiwan Area Mesoscale Experiment (TAMEX) IOP-2 [21]; the formation of the dryline, and the interactions among the nocturnal LLJ, soil moisture, vertical wind shear, and the slope of terrain near the dryline over the Great Plains [2], winter cyclogenesis over the Rocky Mountains [3]. The model has also been used to study the squall line and mesoscale convective system during SESAME [11], and cyclogenesis [22]. The results show that this model can successfully simulate the real atmosphere under various environments. The detailed description of the current version of the PMM is referred to [3].

## 3. Numerical Results and Discussion

It is well known that the numerical weather predictioin is an initial and boundary value problem. The initial and boundary conditions are provide by the PMM objective analysis package. The standard data sets used in the package include the European Center for Medium-Range Weather Forecasts (ECMWF) gobal advanced operational upper-air spectral analysis and surface analysis, the 10-min resolced U. S. Navy global elevation data, the 1 degree resolved Reynold's NMC CAC weekly sea surfcae temperature data, and the 1 degree resolved Henderson-Seller's global vegetation and soils data. The lateral boundary condition is also updated by interpreting the every six-hourly ECMWF analysis at the later boundary. ECMWF analyses at 0000 Z, June 1 1988 are used as the initial conditions. The initial temperature, geopotential, mixing ratio, and wind vector at 500 mb (the mid-level of the atmosphere) are shown in Figs. 2a-d.

The simulation was started at 0000 Z 1 June and integrated for one month. For numerical stability, the small time interval used in this study was 200 sec. After 30 days' integration without nudging, the simulated temperature, geopotential, moisture, and wind vtcor at 500 mb are shown in Figs. 3a-d. They are comparable to the observations, shown in Figs. 4a-d.

The simulated monthly mean fields (Figs. 5a-d) shown a well developed warm ridge over the over north America, and deep troughs developed along east and west coasts. The persistent warm ridge over the north America

effectively blocked the moisture supply from the Gulf of Mexico and resulted in a severe drought during June of 1988. The humidity is very low over Mississippi Valley and west Pacific Ocean. They are also in good agreement with observations (Figs. 6a-d).

## 4. Summary

This preliminary results show the PMM can reproduce the observed weather pattern of June 1988 very well. It is also proved that this model can be an important tool to study the regional climate change and water cycle in a time scale of month over a large continent. It is well known that the numerical weather prediction models require huge computer CPU, memory, and disk space. The PMM was developed under CYBER 205 supercomputer enviroment. Recently, we have modified the model to run in a IBM SP2 parallel computing machine. For this simulation it took 800,000 sec CPU time (IBM/RISC-590 processor), 128 megabytes RAM, and 3 gigabytes of data storage.

## 5. Acknowledgements

This work was sponsored by a grant from the IBM Environmental Research Program, directed by Dr. Joseph Sarsenski, by the NSF under grants ATMS-9213730 and ATMS-8907881, and by the Department of Energy under grant IU/DOE 21312-0054.

## 6. References

1 Sun, W.Y., J.D. Chern, C.C. Wu, and W. R. Hsu, 1991: Numerical simulation of mesoscale circulation in Taiwan and surrounding area. Mon. Wea. Rev. 119, 2558-2573.

2 Sun, W. Y., and C. C. Wu, 1992: Formation and diurnal oscillation of dryline. J. Atmos. Sci., 49, 1606-1619.

3 Chern, Jiun-Dar, (August, 1994) Numerical simulation of cyclogenesis over the western United States. Ph.D. thesis, Purdue University, 178 pp.

4 Bosilovich, M. G., and W. Y. Sun, 1994: Formation and Verification of a land surface parameterization for atmospheric models (Boundary Layer Meteorology, in press).

5 Businger, J. A., J. C. Wyngaard, Y. Izumi, and E. F. Bradley, 1971: Flux-profile relationships in the atmospheric surface layer. J. Atmos. Sci., 28, 181-189.

6 Sun, W. Y., 1993 a: Numerical simulation of a planetary boundary layer: Part I. Cloud-free case. Beitrage zur Physik der Atmosphare, 66, 3-16.

7 Sun, W. Y., 1993 b: Numerical simulation of a planetary boundary layer: Part II. Cloudy case. Beitrage zur Physik der Atmosphare, 66, 17-30.

8 Wu, C.-C., and W. Y. Sun, 1990a: Diurnal oscillation of convective boundary layer. Part I: Cloud-free Atmosphere. Terrestrial, Atmospheric and Oceanic Sciences, 1, 23-43.

9 Wu, C.-C., and W. Y. Sun, 1990b: Diurnal oscillation of convective boundary layer. Part II: Cloudy Atmosphere. Terrestrial, Atmospheric and Oceanic Sciences, 2, 157-174.

10 Sun, W. Y., and W. R. Hsu, 1988: Numerical study of cold air outbreak over the warm ocean. J. Atmos. Sci.,45.,1205-1227.

11 Haines, Patrick A., (May, 1992): Numerical simulation of a squall line: Tests of a new cumulus paramet-erization scheme. Ph.D. thesis. 395 pp.

12 Molinari, J., and T. Corsetti, 1985: Incorporation of cloud-scale and mesoscale downdrafts into a cumulus parameterization. Results of one and three dimensional integrations. Mon. Wea. Rev., 113, 485-501.

13 Gadd, A. J., 1978: A split explicit integration scheme for numerical weather prediction. Quart. J. Meteor. Soc., 104, 569-582.

14 Sun, W. Y., 1980: A forward-backward time integration scheme to treat internal gravity waves. Mon. Wea. Rev., 108, 402-407.

15 Sun, W. Y., 1984: Numerical analysis for hydrostatic and nonhydrostatic equations of inertial-internal gravity waves. Mon. Wea. Rev., 112, 259-268.

16 Sun, W. Y. , 1995: Calculating pressure gradient in a sigma coordinate (submitted for possible publication)

17 Sun, W. Y., 1993c: Numerical experiments for advection equation. J. of Comput. Phys., 108, 264-271.

18 Hsu, W.-R., and W. Y. Sun, 1991: Numerical study of mesoscale cellular convection Boundary-Layer Meteorol. 57, 167-186.

19 Sun , W. Y., and J. D. Chern, 1993: Diurnal variation of lee-vortexes in Taiwan and surrounding area . J. Atmos. Sci. 50, 3404-3430.

20 Sun, W. Y., and J. D. Chern, 1994: Numerical experiments of vortices in the wake of idealized large mountains. J. Atmos. Sci., 51, 191-209.

21 Hsu, W. R., and W. Y. Sun, 1994: A numerical study of a low-level jet and its accompanying secondary circulation in a Mei-yu system. Mon. Wea. Rew. 122, 324-340.

22 Yildirim, Ahmet, (May, 1994) Numerical study of an idealized cyclone evolution and its sub- synoptic features. Ph.D. thesis, Purdue University, 145 pp.

23 Chagnon, S. A., 1989: The 1988 drought, barges, and diversion. Bull. Amer. Meteor. Soc., 70, 1092-1104.

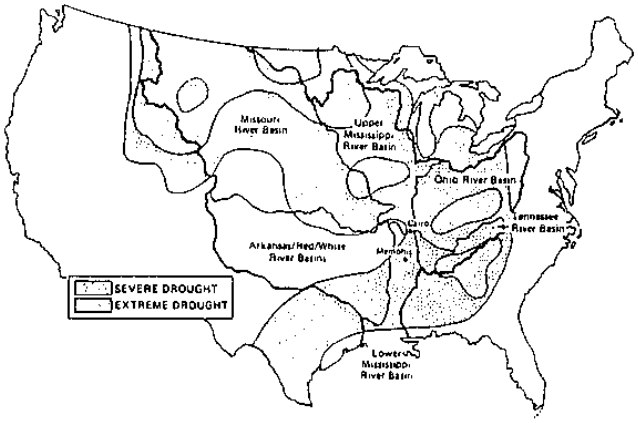


Fig. 1 The areas of severe drought in the Mississippi River Basin on 15 June 1988 [23].

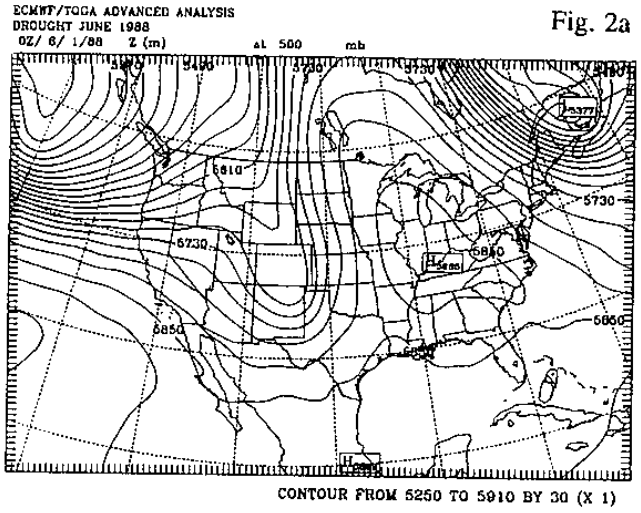


Fig. 2a

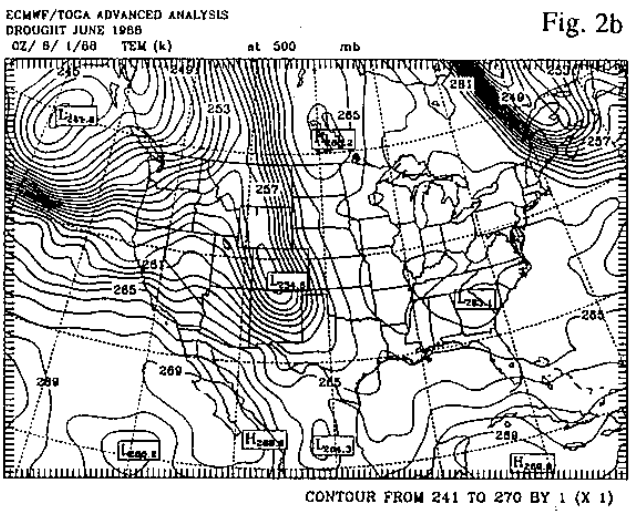


Fig. 2b

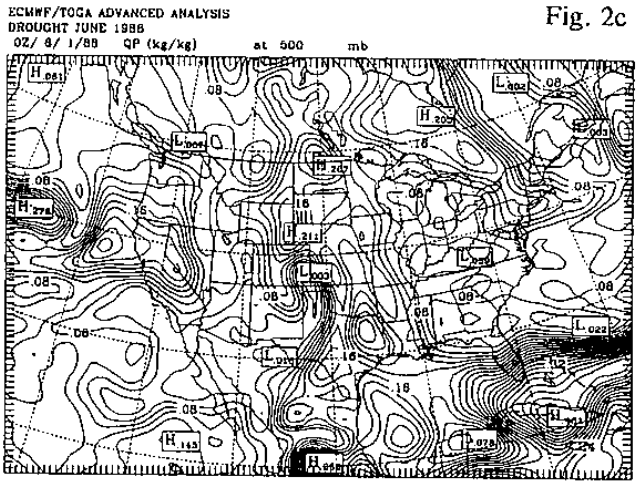


Fig. 2c

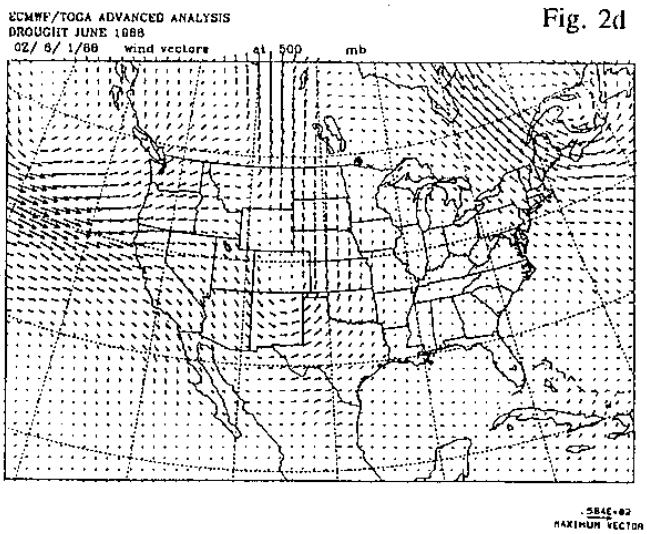


Fig. 2d

Fig. 2 ECMWF/TOGA advanced analysis at 500 mb at 00Z 1 June: (a) geopotential, (b) temperature, (c) mixing ratio $q_v$, and (d) wind vector.

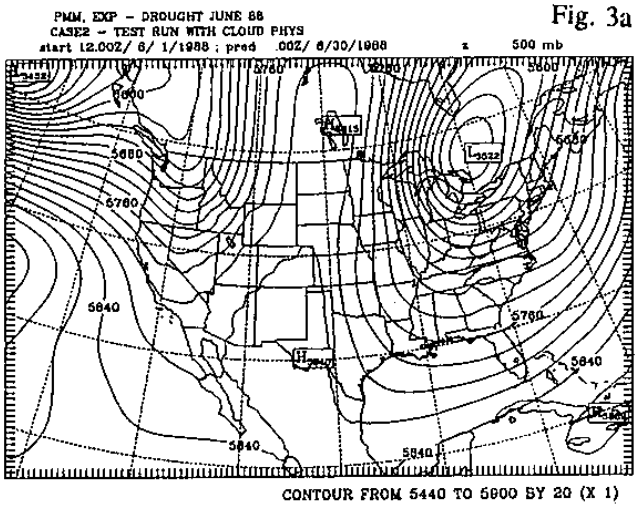


Fig. 3a

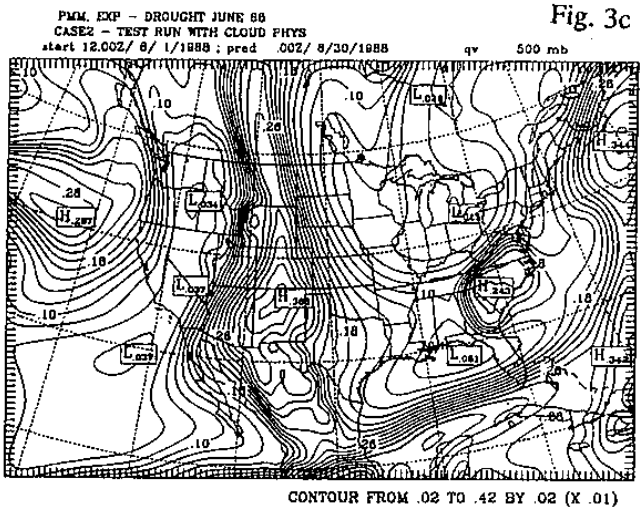


Fig. 3c

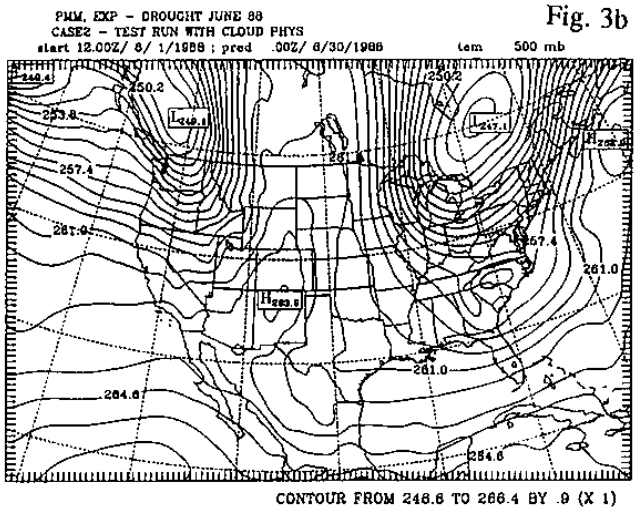


Fig. 3b

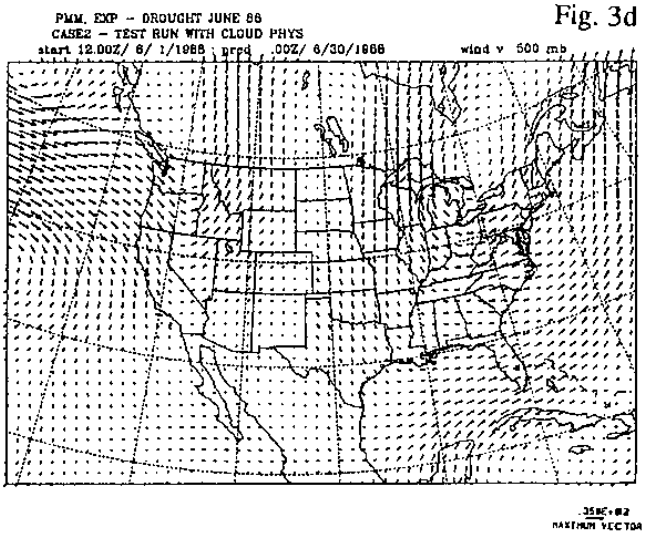


Fig. 3d

Fig. 3 Simulations at 500 mb at 00Z 30 June (a) geopotential, (b) temperature, (c) mixing ratio $q_v$, and (d) wind vector.

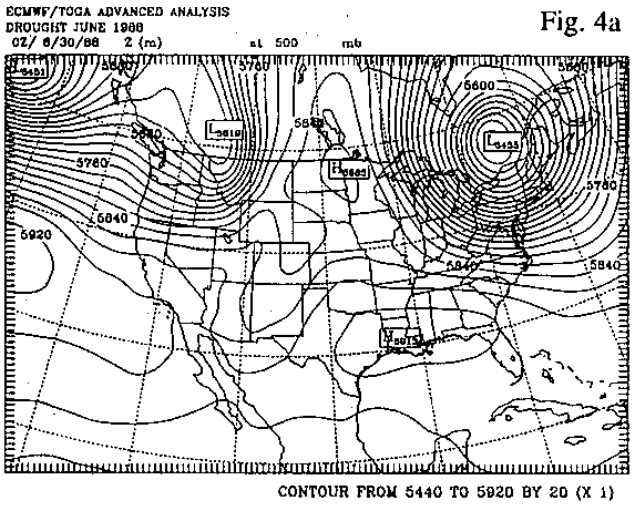


Fig. 4a

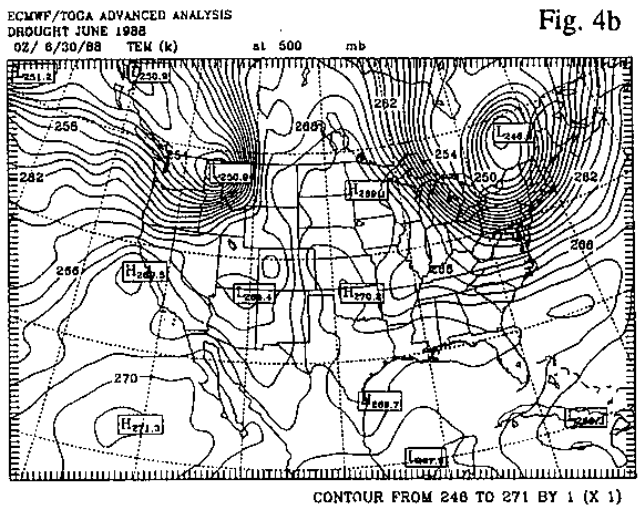


Fig. 4b

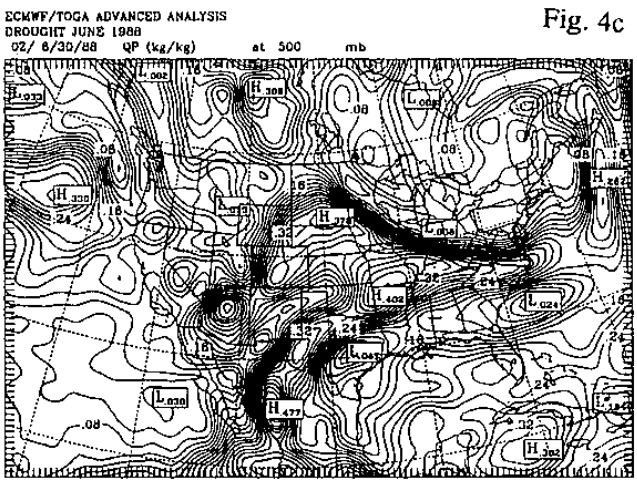


Fig. 4c

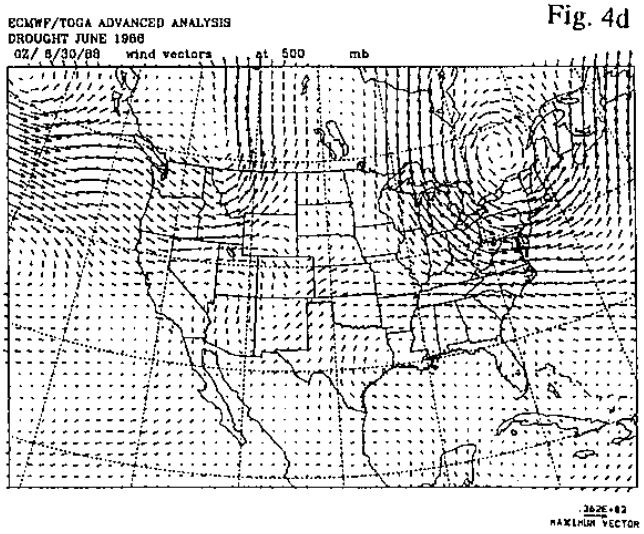


Fig. 4d

Fig. 4 ECMWF/TOGA advanced analysis at 500 mb at 00Z 30 June (a) geopotential, (b) temperature, (c) mixing ratio $q_v$, and (d) wind vector.

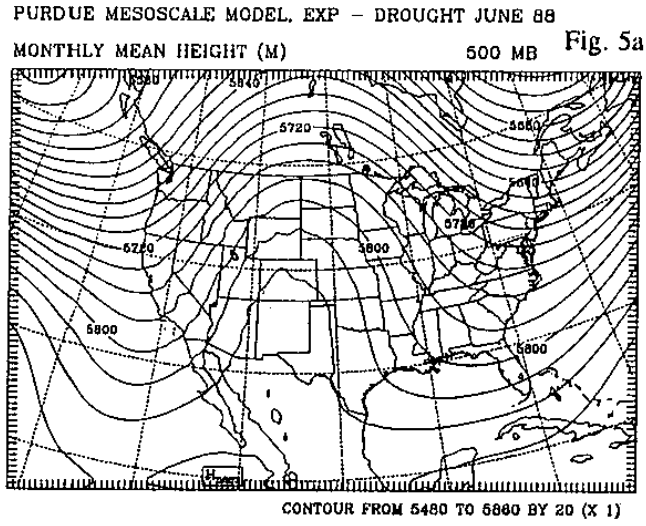


Fig. 5a

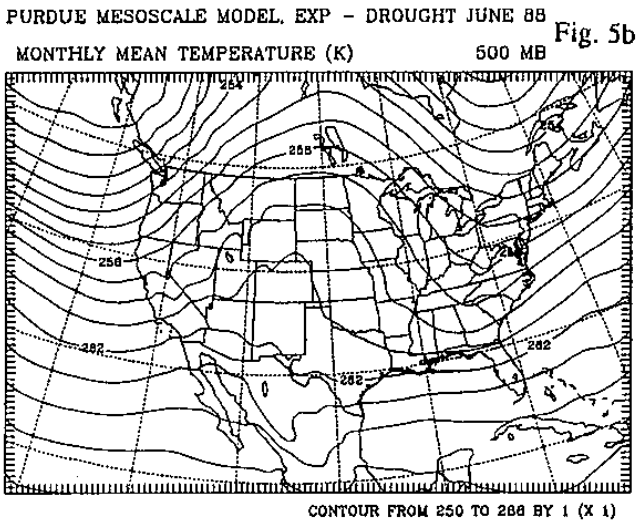


Fig. 5b

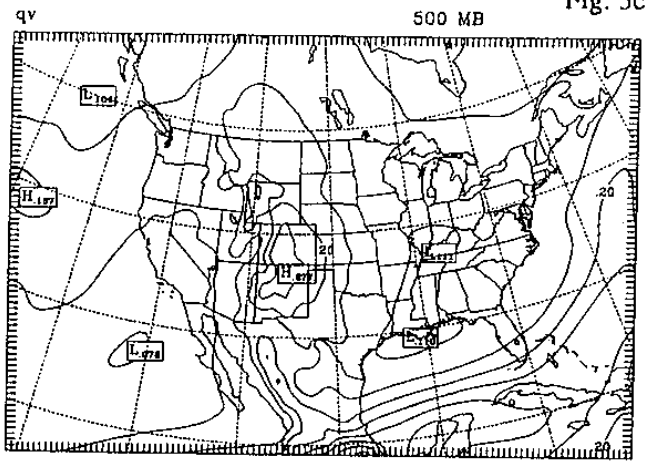


Fig. 5c

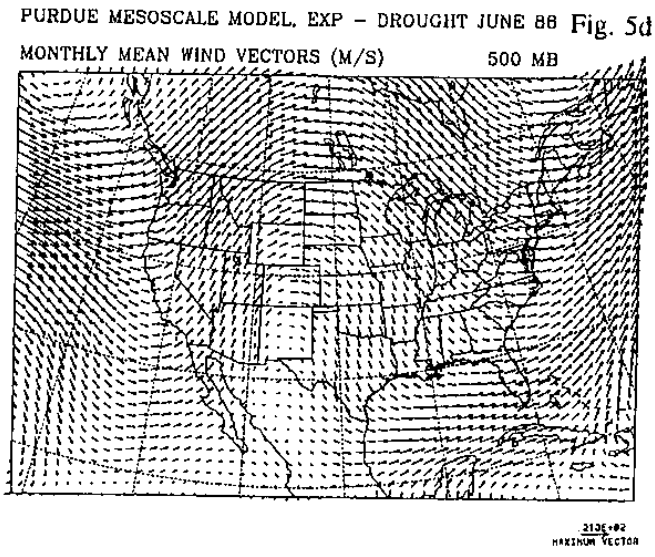


Fig. 5d

Fig. 5 Simulated montly mean at 500 mb for June 1988 (a) geopotential, (b) temperature, (c) mixing ratio $q_V$, and (d) wind vector.

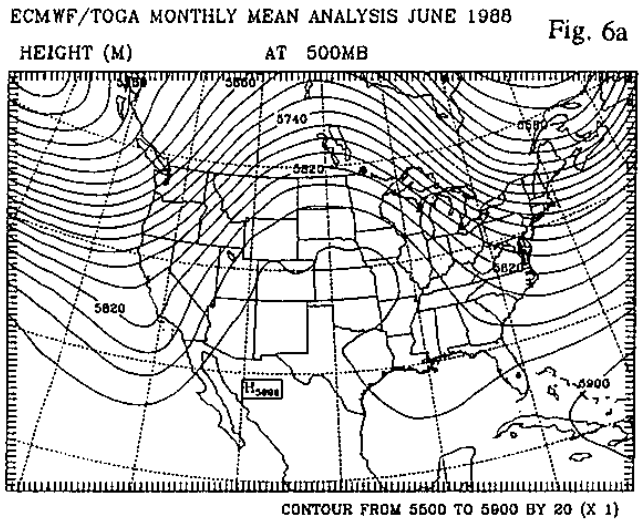


Fig. 6a

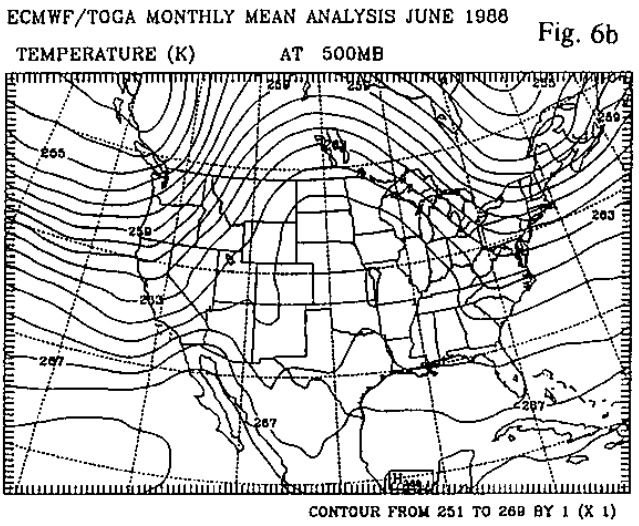


Fig. 6b

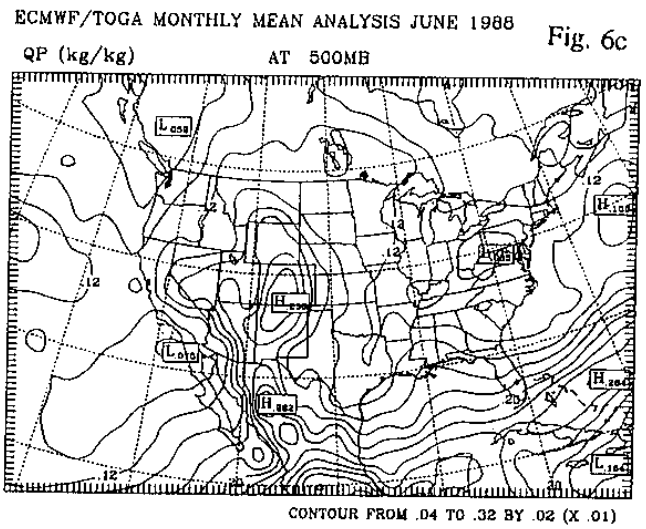


Fig. 6c

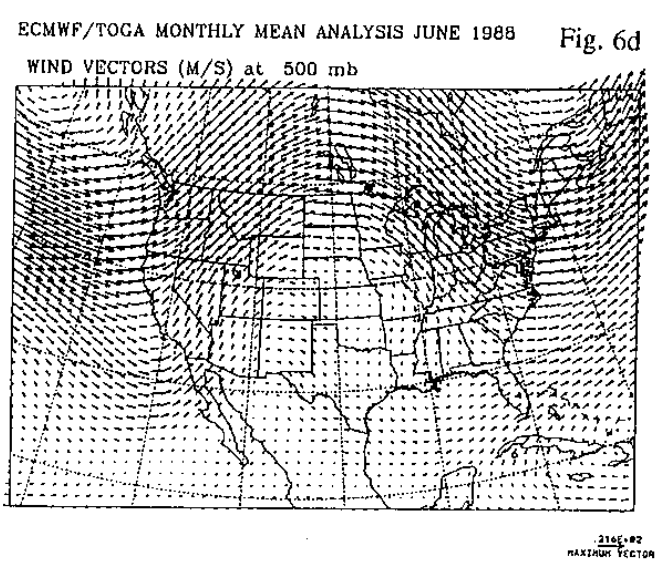


Fig. 6d

Fig. 6 ECMWF/TOGA monthly mean at 500 mb for June 1988 (a) geopotential, (b) temperature, (c) mixing ratio $q_v$, and (d) wind vector.